

ANALYSIS ON THE EFFECT OF BURIED DEPTH-INITIAL WATER CONTENT OF THE TUNNEL IN EXPANSIVE ROCK

Li Xinyu¹, Chen Wei², Cao Pan² and Zhang Huijian²

1. *The 2nd Engineering Co. Ltd of China Railway 12th Bureau Group, Taiyuan 030000, China; 3692384151@qq.com*
2. *Southwest Jiaotong University, Key Laboratory of Transportation Tunnel Engineering, Ministry of Education, Chengdu, No. 111, North Section, Second Ring Road, Jinniu District, 610031, China; 962246504@qq.com; 305434884@qq.com; huijianz@163.com*

ABSTRACT

There are countless engineering disasters induced by expansive strata in the tunnel project. Nowadays, most of the research focuses on the basic characteristics of expansive rock and soil, while the influence about coupling buried depth and different initial water content of surrounding rock on the tunnel lining is still rarely involved. Based on the principle of temperature and humidity equivalence, this paper discusses the behavior of rock as well as the mechanical properties of lining under the interaction of different buried depth and initial water content by using FLAC^{3D} numerical simulation. It was found that the initial water content shows an obvious effect on the evolution about the plastic area of rock compared with the buried depth of the tunnel. For shallow tunnels with a water content of less than 10 %, the plastic zone of the vault will penetrate to the surface after water absorption and expansion. Under the coupling effect, buried depth inhibits the development of the plastic zone to a certain extent. For different initial water contents of the surrounding rock, the displacement of the tunnel adds with the burial depth. The swelling of rock will significantly reduce the safety of the primary support, and when the burial depths of the tunnel increase to 150 m, the security coefficients of some primary support structures are less than 2, which does not meet the need in standard. The safety factor of secondary support is mainly influenced by the expansion force, not the ground pressure (represented by buried depth). The findings may be valuable reference for the analysis as well as evaluation of the security as well as stability of tunnels in expansive mudstone.

KEYWORDS

Expansive rock, Mechanical properties, Deformation law, Tunnel, Water content, Buried depth

INTRODUCTION

Expansive rocks are widely distributed all over the world. With the continuous development of transportation hubs, tunnel lines inevitably cross expansive rock strata [1, 2]. As a typical expansive rock, mudstone has complex engineering properties, namely, due to its rich in hydrophilic minerals, it is prone to water swelling and water loss shrinkage [3]. The deformation and mechanical behavior of tunnels have always been the focus of attention [4, 5]. In the expansive rock strata faced by practical engineering, the stress property of the original rock after disturbance under various in-situ stress levels (buried depth) is often ignored. So it remains paramount meaning to investigate the tunnel in expansive rock under the influence of different in-situ stress levels and initial water contents.

According to the International Society of Rock Mechanics (ISRM), expansive soft rock is defined as a low-strength engineering rock mass containing highly expansive clay minerals and

undergoing significant deformation at low-stress levels. Some studies have investigated the mechanical characteristics of expansive rock specimens [6], and some scholars have also studied the construction mechanical properties of tunnels in the expansive surrounding rock. Alonso et al. [7] revealed that the extreme expansion phenomenon in the construction and later operation process of Lila tunnel was due to the existence of anhydrite and water circulation around the surrounding rock, and then the tunnel section shape was changed and reinforced concrete lining was applied to resist the expansion pressure. Based on the convergence constraint method and empirical method, Zhu et al. [8] proposed a stability analysis and calculation method of tunnels considering expansion pressure and for different types of expansive rock. Ma et al. [9] studied the mechanical effect of water absorption and expansion of soft rock in the excavation process of tunnel, and found that the damage degree of surrounding rock in the process of tunnel excavation is very small, and the support resistance is the important factor limiting the tunnel bottom deformation and the stability of surrounding rock. Chen et al. [10] regarded the swelling phenomenon of the weak rock around the tunnel as a humidity-stress coupling process and obtained the stress and displacement solutions of the high expansion potential of the tunnel. Considering the expansion stress and shear expansion, the variation trend of the plastic area as well as the deformation of the surrounding rock were obtained. Chen et al. [11] obtained the displacement as well as mechanical properties of the tunnel in expansive rock before and after the tunnel humidification by simulating the humidity field through the temperature field. At the same time, the orthogonal test analysis showed that the most vital factors affecting the tunnel were the humidification strength, followed by the buried depth-span ratio, expansion thickness, and expansion coefficient. Zhao et al. [12] carried out the impact of tunnel basement swelling on the deformation and stress of tunnels in mudstone under various water content conditions. The basement expansion had a great influence on the bottom drum of the bottom part and had some resistance influence on the vault deformation. Liao [13] reveals that the shear strength of rock around the tunnel is significantly weakened because of the augmentation of water content, which is the main factor to bring about the deformation and instability of the tunnel. Considering the effect of surrounding rock expansion and strength deterioration, the variation law of displacement of tunnel lining structure is obtained. From the existing research on tunnels in expansive rock, the deformations as well as stress properties of the tunnel in expansive rock have been studied, but most of the factors considered are the initial water content, expansion as well as contraction, swelling softening and expansion range of expansive surrounding rock [14-16]. There is no systematic study on the difference in mechanical properties of tunnel in swelling rock under different initial water content and stress levels of surrounding rock.

Therefore, based on the tunnel project in swelling mudstone, this paper adopts the numerical simulation method and considers different buried depths and initial water content to simulate the expansion of mudstone based on the principle of temperature and humidity equivalence. The deformation rule as well as the stress evolution mechanism of tunnels in expansive mudstone are revealed.

PROJECT BACKGROUND

The relied tunnel project is one of the railway tunnel located in northern China. The largest burial depth of the tunnel is around 125 m. The size of tunnel is listed in Figure 1. The tunnel mainly crosses through mudstone, sandstone, and gneiss, the surrounding rock grade is V (poor condition). No surface water is found in the region where the tunnel crosses through, while the water in the connection region between basalt as well as mudstone is enriched, showing the nature of stagnant water in the upper layer. No groundwater was found during the survey, and there was a small amount of water seepage.

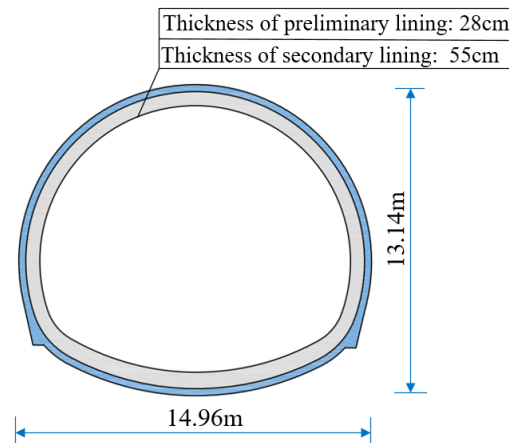


Fig. 1 – Tunnel section diagram

The research area in this paper is mainly aimed at tunnels passing through expansive mudstone sections. Combined with the previous basic characteristics test of the surrounding rock (mudstone) by this research group [17, 18], it is found that it has significant expansibility, and the montmorillonite content is as high as 26.4%, and the average free expansion rate is as high as 53.5%. Combined with other indicators, the surrounding rock in this area is determined to be moderately expansive potential according to the standard [19]. Because mudstone has the characteristics of water expansion and softening, if its expansion characteristics are not fully considered in design and construction, it may lead to a series of engineering diseases (such as cracking of preliminary lining, deformation invasion, etc.), and even tunnel collapse in severe cases.

NUMERICAL CALCULATION INSTRUCTION

Calculation model

Referring to the site construction and design scheme, the height as well as width of the tunnel model are selected as 13.14 m and 14.96 m, respectively. To reduce the impact of boundary effects, 3 ~ 5 times the diameter of the tunnel is generally taken around the tunnel. To facilitate the calculation speed, the distance from the left as well as right sides about the tunnel to the tunnel's boundaries is 4 times the tunnel diameter. The space from the lower boundaries to the inverted arch is three times the tunnel diameter. Finally, the length and width of the calculation model are determined as 130 m and 50 m, and the height of the model varies according to the selected buried depth. Combined with the actual tunnel burial depth and research needs, the tunnel burial depths are set to 30m, 75m, 125m, 150m and 200m respectively. Normal constraints are imposed on the front, rear, left, and right as well as lower boundaries of the model, while the top boundaries are set to free [20, 21].

The calculation model is displayed in Figure 2. Among them, the 30 m and 75 m buried depth models are modeled according to the actual depth. To facilitate the calculation, the buried depth condition of 125m ~ 200m is realized by applying equivalent self-weight stress to the upper interface of the 75m buried depth model. The excavation scheme of the tunnel is consistent with the construction site, and the step method is adopted for excavation. The temporary inverted arch is constructed after the excavation of the middle steps as well as the upper steps of tunnel. The temporary inverted arch material is I18-type steel, the shotcrete thickness is 10 cm, and the excavation and support cycle footage of tunnel is 1.8 m.

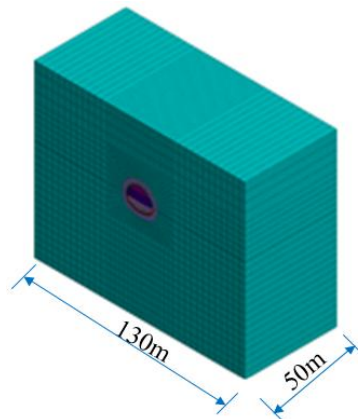


Fig. 2 – Calculation model

Calculation parameters

The lining structure as well as rock is realized through solid elements. Among them, the rock adopts the Mohr-Coulomb yield criterion, while support adopts linear elastic constitutive model. The design parameter of the support is shown in Table 1. Note: Table 1 is obtained through on-site geological investigation and design material of the relied project.

Tab. 1 - Lining type and parameter

Surrounding rock classification	Design lining type	Preliminary lining			
		Shotcrete	Shotcrete thickness /cm	Steel frame model	Spacing /m
V	V _{p1} composite lining	C25	28	I20a	0.6
Secondary lining					
Reinforced concrete		Filled layer concrete		Arch wall thickness /cm	Invert thickness /cm
C35		C20		55	65

The primary support for tunnel adopts C25 shotcrete (28 cm thick), and the steel arch adopts an I20 steel frame. The effect of steel frame in primary support is transformed to shotcrete by the elastic modulus. The calculating formula [22] is as Equation (1):

$$E = E_0 + \frac{S_g E_g}{S_c} \quad (1)$$

Where, E represents the calculated elastic modulus of concrete; E_0 represents the elastic modulus of original concrete; S_g represents the cross-sectional area of steel arch; E_g represents elastic modulus of steel; S_c represents the cross-sectional area of concrete.

Combined with the on-site geological investigation and design material of the relied project, the final adopted calculation parameter of rock and support structure is listed in Table 2.

Tab. 2 - Calculation parameter of rock and support structure

Material name	Density /(kg/m ³)	Elastic modulus <i>E</i> /MPa	Poisson ratio <i>v</i>	Cohesion <i>c</i> /MPa	Internal friction angle <i>φ</i> /°
Primary support	2500	33100	0.2	-	-
Secondary support	2500	31500	0.2	-	-
Rock	2100	367	0.38	0.264	31

On the strength of expansive mudstone after humidification and saturation, combined with the literature [14, 23, 24] and considering that the mudstone of this project has stronger expansibility and lower strength, the softening degree of *E*, *c* and *φ* about mudstone under different initial water content are proposed to be 0.5, 0.7 and 0.45. According to the empirical equation of the previous study and the relevant test results [25, 26], combined with the mechanical index properties of expansive rock around tunnel in this project, a certain degree of reduction is carried out, the softening strength parameters of expansive mudstone after water absorption saturation suitable for each initial water content of this project are obtained [17], as listed in Table 3.

Tab. 3 - Softening strength parameters of expansive rock after water absorption saturation

Initial water content /%	<i>E</i> /GPa	<i>v</i>	<i>c</i> /kPa	<i>φ</i> /°
5	0.379	0.33	265	17.3
10	0.184	0.38	216	14.6
15	0.099	0.41	167	13.1
20	0.060	0.44	117	11.6
25	0.042	0.45	68	11.1

Implementation of swelling behavior

Because the material thermal swelling properties of temperature field are consistent with the numerical expressions of the water swelling properties of the expansive soil, the humidity field may be realized using temperature field through parameter conversion. Through the thermal-mechanical coupling analysis module in the numerical software, the deformation as well as stress properties of expansive soil can be got if humidity in the soil changes. Based on the thermal swelling equations of thermodynamics [27, 28], it can be represented by Equation (2):

$$\Delta \varepsilon_{ij} = \alpha \Delta T \delta_{ij} \quad (2)$$

Where, α represent thermal expansion coefficient; ΔT represents strain increment led by temperature change; δ_{ij} represents Kronecker mark.

The impact of humidity on deformation equations about expansion soil is expressed as follows [27, 28]:

$$\Delta \varepsilon_{ij}^{\omega} = \beta \delta_{ij} \Delta \omega = \beta \delta_{ij} C_{\omega} \Delta u \quad (3)$$

Where, $\Delta\varepsilon_{ij}^{\omega}$ is the increment of rock mass strain caused by humidity change; β represents humidity expansion coefficient; $\Delta\omega$ represent the change in water content of rock per unit volume.

The correlation between thermal swelling coefficient and humidity swelling ratio can be got by combining Equation. (2) and Equation. (3):

$$\alpha = \frac{\beta\Delta\omega}{\Delta T} = \frac{\beta C_{\omega}\Delta u}{\Delta T} \quad (4)$$

Therefore, in the case of assuming the temperature changing values, by deciding the temperature linear swelling ratio corresponding to the humidity linear swelling ratio, the temperature stress field can be realized to implement humidity stress field. Once the change in the humidity field of rock is known, the temperature field can be established by using the above equations, so that the temperature stress field in the calculation tool can be used to approximately simulate the expansion characteristics of the surrounding rock about tunnel in swelling rock. On the basis of the thermal expansion effect of material heating, the temperature module in FLAC3D is used to realize the process of water absorption and swelling of rock. The solution and verification process of specific temperature field expansion parameters can be referred to literature [17], and the used temperature field swelling parameter is listed in Table 4.

Tab. 4 - Temperature field calculation parameters

ω_0 /%	β	ΔT /°C	α
5	0.0046	100	0.0011
10	0.0044	100	0.0009
15	0.0042	100	0.0006
20	0.0038	100	0.0004
25	0.0026	100	0.0001

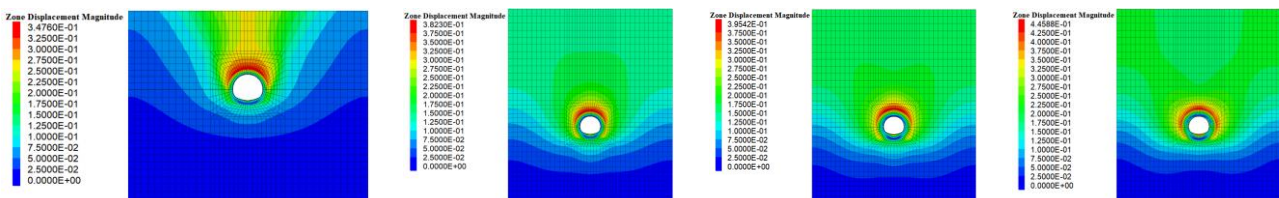
ANALYSIS OF CALCULATION RESULTS

The time of expansion of expansive rock may occur in the closed-loop stage of preliminary support (i.e., before the installation of secondary support), or the completion stage of secondary support installation. Therefore, this section discusses these two conditions.

Influence of rock expansion before secondary support installation

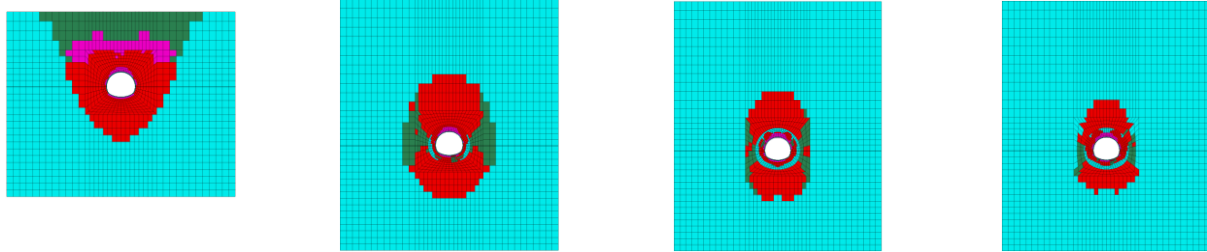
Distribution law of deformation as well as plastic zone about rock

Taking the initial water content (5%) of rock as an example, the deformation as well as plastic zone of rock after water absorption to saturation expansion under various burial depths of tunnel are displayed in Figure 3 and Figure 4, respectively.



(a) 30m (b) 75m (d) 150m (e) 200m

Fig. 3 – Displacement distribution law of rock under various burial depths



(a) 30m (b) 75m (d) 150m (e) 200m

Fig. 4 – Distribution law about plastic zone of rock under different buried depths

In Figures 3~4, the displacement of rock adds and the plastic zone decreases with the burial depth of tunnel. For the plastic zone diagram of rock, the tensile invalidity plastic zones are red and green, while shear invalidity plastic zone is red. For case of tunnels with shallow buried depth, the swelling of rock is relatively more dangerous. Taking the buried depth of 30 m as the case, after the expansion of surrounding rock, the plastic zone runs through the surface. The largest displacement about rock reaches 347 mm. On the one hand, the deformation of the rock causes the support structure to carry much surrounding rock pressures. On the other hand, it will also expand the scope of the expansion zone. The expansion of rock shows the greatest influence on the evolution of plastic zone of vault. When the buried depth increases to 75 m, the plastic zone of vault does not develop to the surface. Therefore, it can be inferred that under the most unfavorable conditions, the largest development depth about vault plastic zone is nearly 3 times tunnel diameter.

Taking the tunnel burial depth = 150 m as the case, the displacement and plastic zone law of rock after water absorption to saturation expansion under different initial water content is listed in Figure 5 and Figure 6, respectively.

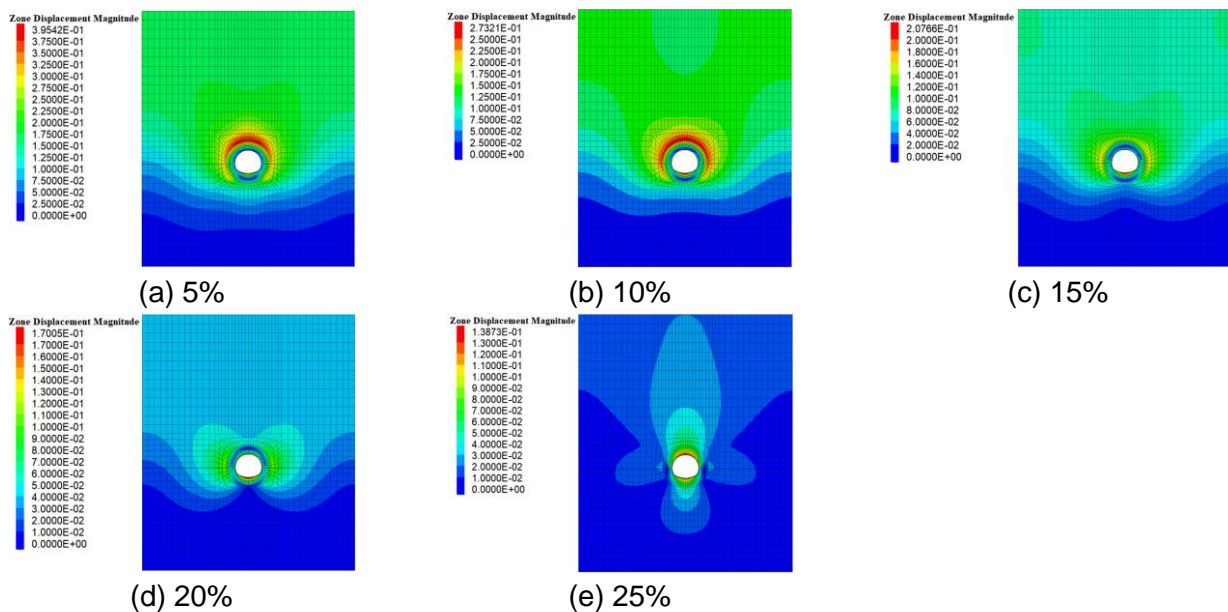


Fig. 5 – Displacement distribution law about rock under different initial water content

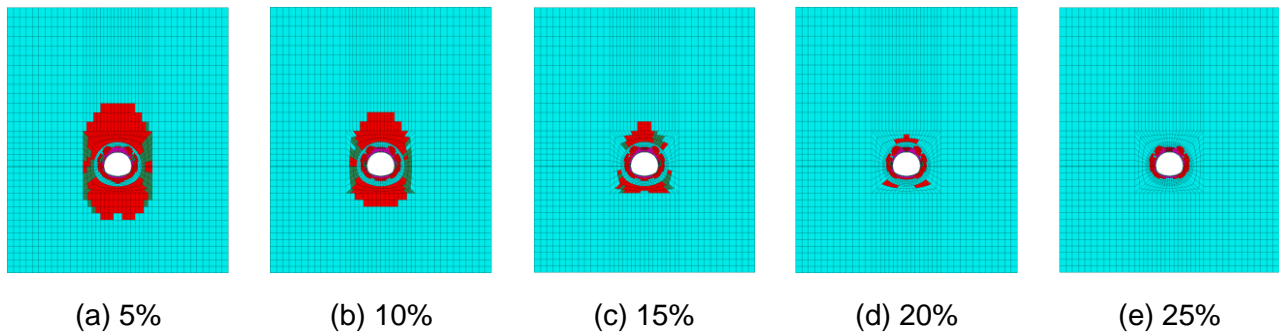


Fig. 6 – Distribution characteristics of plastic zones about rock under various initial water content

In Figs. 5–6, the deformation as well as plastic zone of rock are significantly influenced by initial water content. For the initial water content at 5 % ~ 25 %, the largest deformation of rock is 395mm, 273mm, 207mm, 170mm and 139mm respectively. Combined with the displacement cloud diagram about rock as well as the distribution characteristics of plastic zone, when the initial water content increases to 15 %, the decreases in rock displacement are significantly lower than that of the previous conditions, and the plastic zone area is tended to be stable. The reason may refer to the limited expansion capacity of expansive rock. When the initial water contents of rock are up to a certain degree (close to the expansion capacity about rock), the swelling effect has little impact on the displacement and plastic zones.

The curve of correlation between the initial water content of rock and the volume about plastic zone under various buried depth of tunnels is listed in Figure 7.

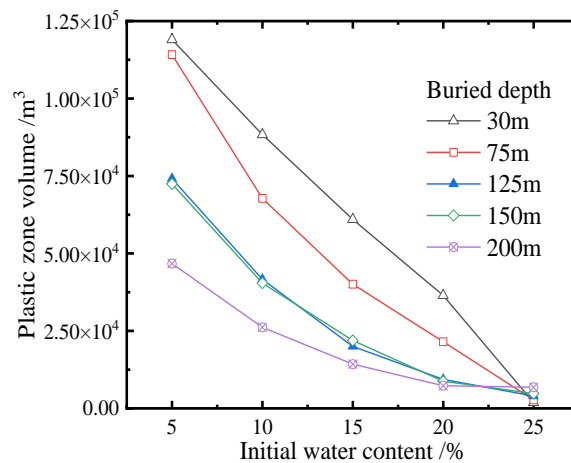


Fig. 7 – Variation in plastic zone volumes about rock with initial water content under various buried depths

In Figure 7, the change rule of plastic zone area about rock under various buried depth is as follows: with the increase of initial water contents, the plastic zone volume about rock decreases gradually, and buried depths can inhibit the development about plastic zone. With the adding of buried depth, the change rate about plastic zone volumes reduces with initial water content. Taking buried depth at 150 m as the case, the plastic zone volume of rock under 5 % ~ 25 % water content is 72435.6 m³, 40420 m³, 21886.9 m³, 8726.3 m³, and 4785 m³, respectively, and the maximum decrease rate is 93 %. When initial water content is larger than 20 % and the buried depth is greater than 75 m, the buried depths are a little sensitive to the change in plastic zone volume. At the same time, the plastic zone volume of all conditions is very close at the initial water content of 25%. This is because when the initial water content increases to a certain extent, the whole surrounding rock is close to its expansion limit and is in a very soft state due to the high

water content. At this time, the increase of buried depth has little influence on the volume of its plastic zone.

Deformation law and mechanical properties of lining structure

To monitor the displacement law of primary support under various initial water content about rock and burial depths of tunnel, several typical surveillance points are set in the vital positions of the primary support, as displayed in Figure 8. Because of the symmetrical structure about tunnel, only the left half of the structure is analyzed.

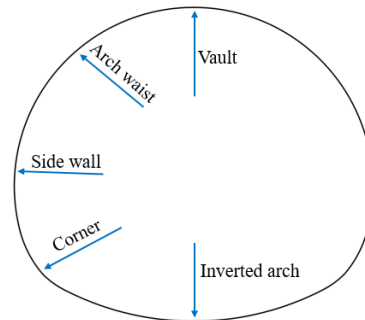


Fig. 8 – Arrangement of monitored points of the displacement of primary support

The relationship curves between the displacement of every monitored point of primary support and initial water content are displayed in Figure 9 after the rock expansion under various buried depths.

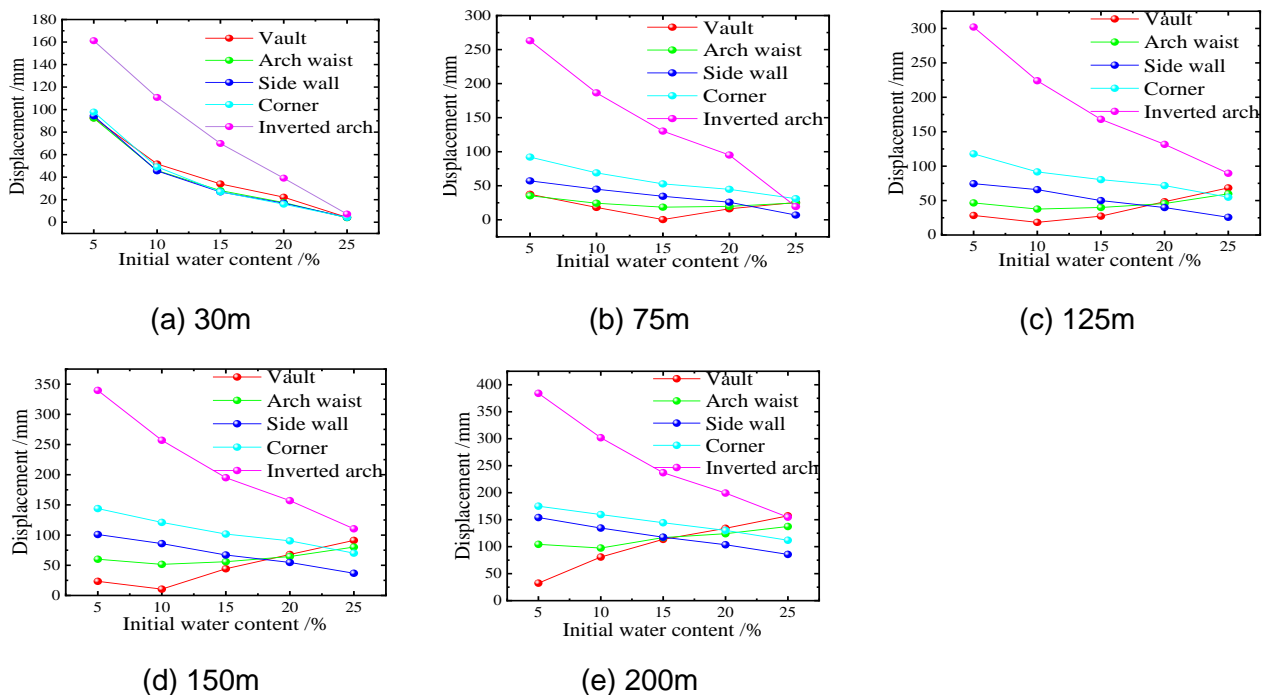


Fig. 9 – Displacement-initial water content curve of each part of primary support under various burial depth of tunnel

In Figure 9, the expansion of surrounding rock shows the greatest impact on deformation of inverted arch. The displacement of inverted arch decreases with the increase of surrounding rock water content, which is basically consistent with the results of the literature [29]. When initial water content is 5 % and the buried depth at 200 m, the deformation value reaches 384 mm. This is because the curvature of the inverted arch is smaller than that of other parts, which is more prone

to deformation. Under the same conditions, when the surrounding rock does not expand, the displacement of inverted arch is 141 mm. The displacement rule of sidewall as well as corner of preliminary lining is consistent with that of inverted arch. The displacement increases with the buried depth and reduces with the decrease of initial water contents. However, the displacement variation of vault and the arch waist is different from that of other parts. This is because the deformation caused by swelling in remaining positions is superimposed on the displacement caused by the previous excavation, while the displacement of the arch waist as well as vault is offset. The reason is that the swelling about rock on both sides of the primary support and inverted arch will lead to the upward uplift displacement of vault, while the expansion about rock above vault will inhibit the upward deformation of the vault. According to the above displacement diagram, the expansion of surrounding rock basically leads to the upward displacement about vault, and the final deformation of primary support of vault is the result of the offset between the settlement caused by the initial excavation and the uplift deformation caused by the expansion. Therefore, in the case of large buried depth (greater than 150m) and the initial water contents are larger than 15 %, the vault shows settlement deformation, which increases with the adding of initial water contents.

Figure 10 is the curve of displacement of each monitored point of primary support with the buried depth of tunnel.

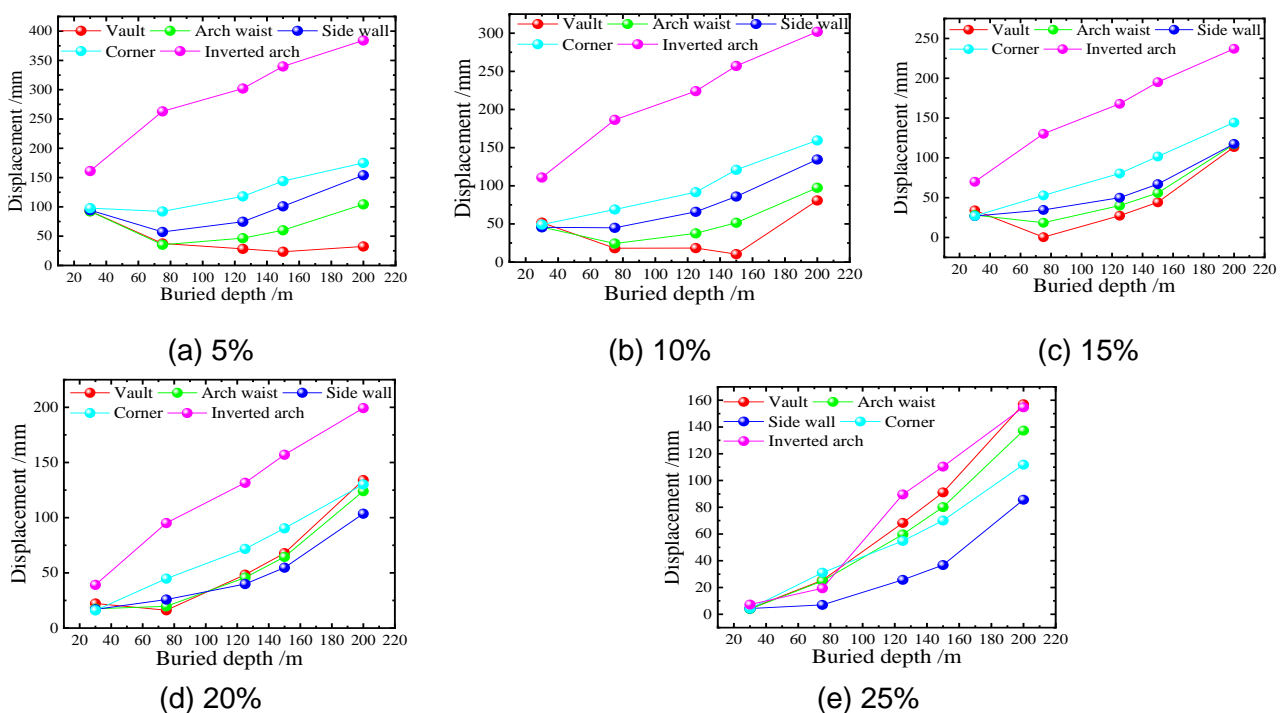


Fig. 10 – Displacement curves of different parts of tunnel under different initial water contents about rock

In Figure 10, under the identical initial water contents, the deformation of each monitoring point after rock swelling shows the characteristics of increasing with buried depth, and the inverted arch is the main deformation position at tunnel. The lower the initial water content, the larger the difference between the deformation of inverted arch and deformation of other monitoring points. And the increase in burial depth inhibits the deformation about monitoring points of the upper half section of the tunnel, especially the lower the initial water contents of rock, the more noticeable the phenomenon. At the same time, with the increase of water content of surrounding rock, the displacement gap between inverted arch and other parts becomes smaller and smaller. This is because when the water content increases to a certain extent, the softening effect of surrounding

rock plays a major role, rather than the expansion effect, resulting in the uplift displacement at the inverted arch becoming smaller and smaller and closer to the displacement at other parts.

Internal force distribution of preliminary lining

Taking the initial water content at 5 % as the case, the bending moments about primary support after the swelling of the rock are extracted, as listed in Figure 11.

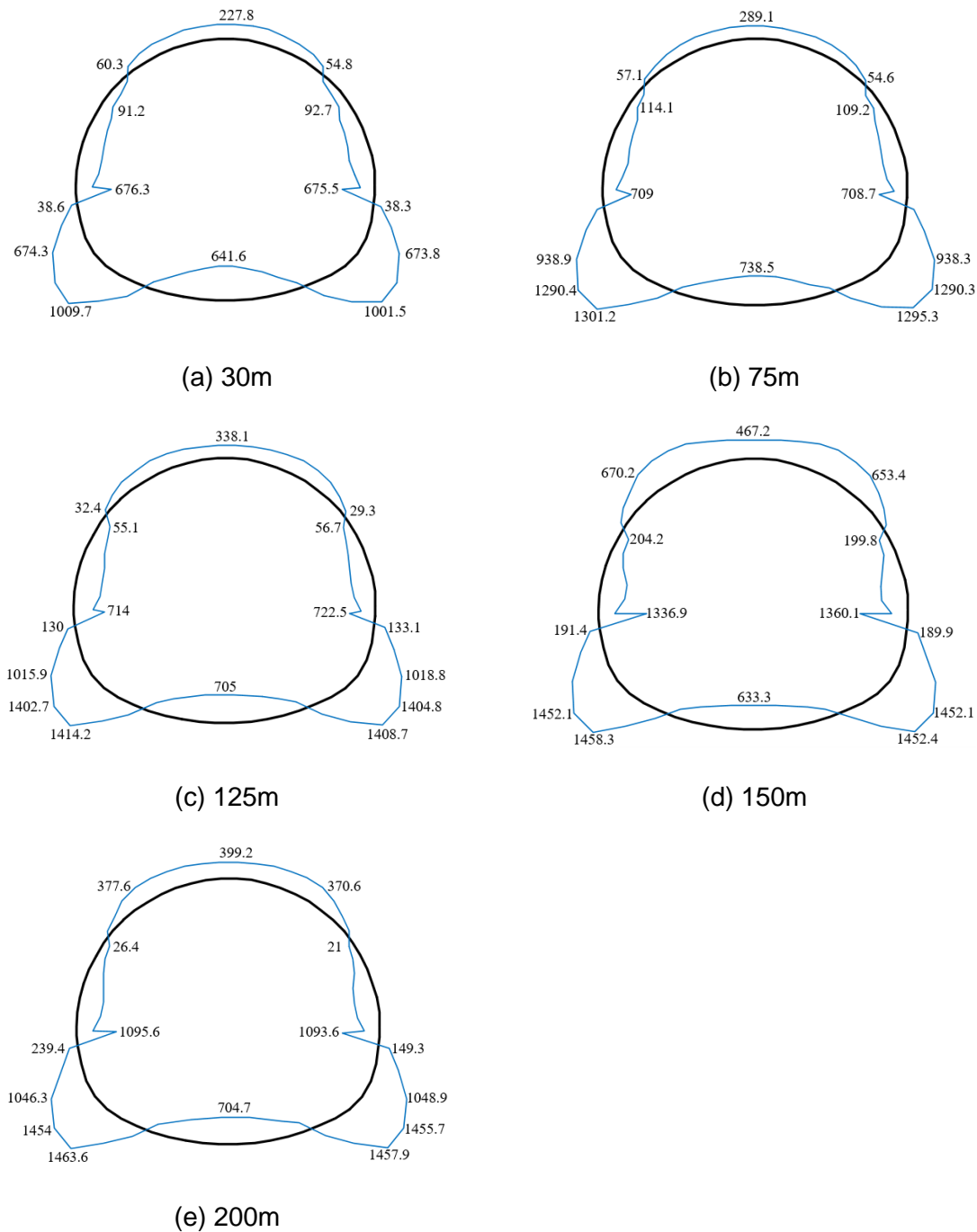


Fig. 11 – Distribution rule of bending moments in primary support at various buried depths after rock swelling

In Figure 11, after the rock expansion, the largest bending moments of primary support occur at the corner. For burial depth at 30 ~ 200 m, with the increase in buried depth, the largest

bending moments at the corner of preliminary lining is 1009.65 kN·m, 1301.15 kN·m, 1414.15 kN·m, 1463.61 kN·m and 1458.27 kN·m respectively. Compared with burial depth condition of 30 m, the bending moment increments of corner under the other buried depth conditions are 293.8 kN·m, 407.2 kN·m, 450.9 kN·m and 456.4 kN·m, respectively. The internal force of tunnel support in expansive rock adds with buried depths, particularly for buried depth at 125 m. When the buried depth increases to 150 m, the burial depth shows little impact on internal force increment of the preliminary lining.

The influence of rock expansion after secondary support installation

The construction concept of the new Austrian method highlights the main bearing objects of load are rock and preliminary support. Secondary support is often considered as the security margin, which can provide a more solid support for the tunnel. As a sudden situation, the expansion of surrounding rock may bring certain risks to the stability of the tunnel. To investigate the stability of secondary support after rock swelling, the bending moments about secondary support under 5 % initial water content and different buried depths are extracted, and safety factors of whole ring secondary support are got. Regarding the calculation method of safety factor, according to the standard [30], the compression intensity of structure members should be determined by Equation (5):

$$KN \leq \varphi \alpha R_a b h \quad (5)$$

Where, K represents safety factor; N represents axial force; R_a is ultimate compression intensity about concrete or masonry; b represents width of cross-section; h represents thickness about cross-section; φ represents the longitudinal bending coefficients about a member, for tunnel support, $\varphi = 1.0$; α represents the eccentricity influencing coefficients about the axial force. According to e_0/h and the table in the code, e_0 represents eccentricity of the axial force.

Starting from the requirements for anti-cracking capacity, the tensile strength about plain concrete rectangular section eccentric compressive member should be calculated according to Equation (6):

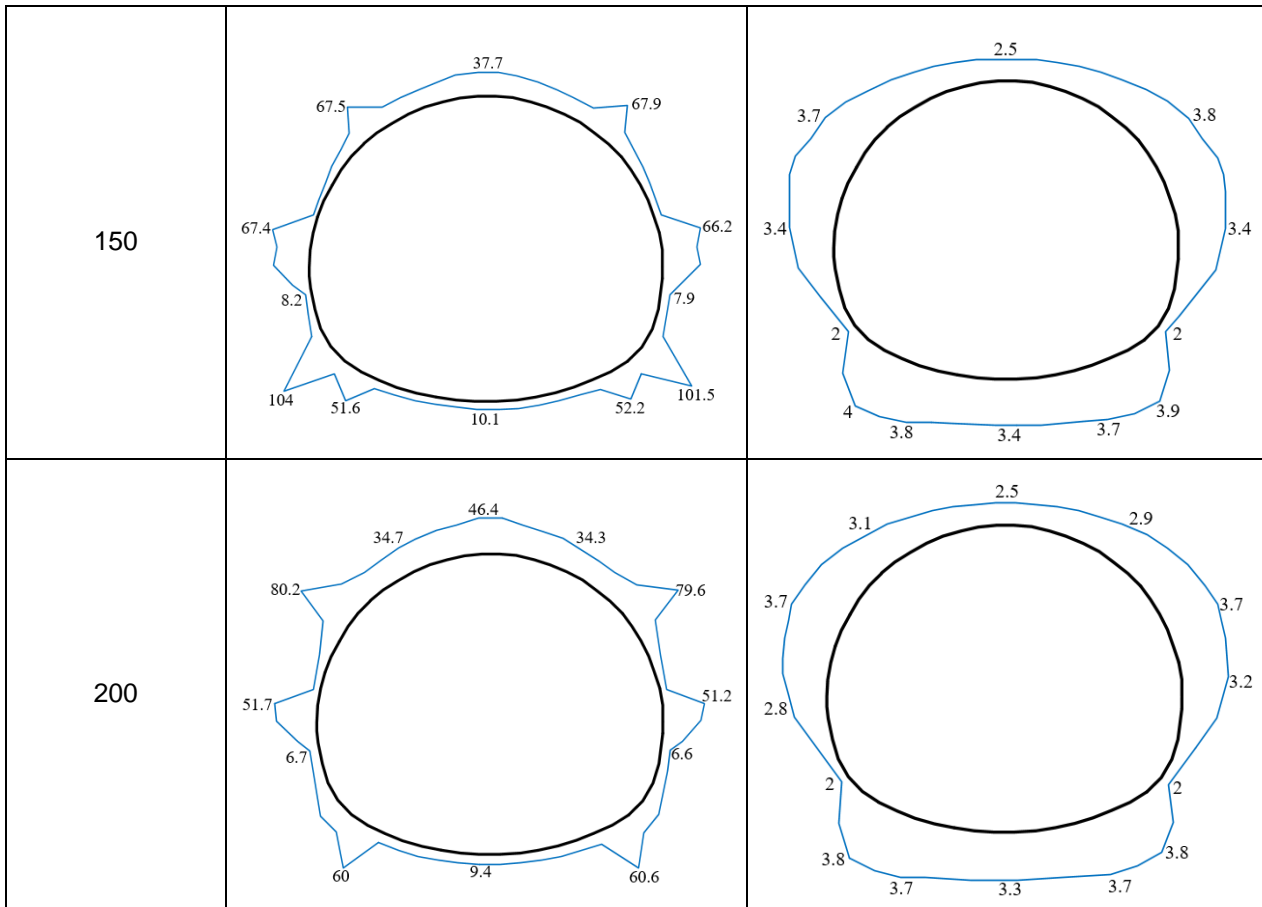
$$KN \leq \frac{1.75 R_1 b h}{\frac{6e_0}{h} - 1} \quad (6)$$

Where, R_1 represents the ultimate tensile intensity about concretes. For concrete rectangular cross-section members, when e_0 is not more than 0.2h, the compression intensity controls the carrying capacities, which is calculated according to Equation (6).

The safety factors of secondary support structure before and after expansion are calculated, as shown in Table 6.

Tab. 6 - Safety factors of secondary support before and after expansion

Buried depth /m	Before expansion	After expansion
30		
75		
125		



It can be seen from Table 6 that if there is no rock expansion, the secondary lining has sufficient safety reserves at all buried depths. When rock expansion occurs, the safety factor of secondary lining is significantly decreased, especially at the corner, which is the weakest site of secondary support. After 150 m buried depth, the safety factors about the corner of secondary support are less than 2, which does not meet the needs in specification.

When the swelling rock distributes around the tunnel, if the expansion occurs in the stage of preliminary lining installation, the expansion effect shows an obvious impact on the displacement of the preliminary support. In particular, the deformation about inverted arch of the tunnel is the largest. The deformation about vault, arch waist, sidewall, and corner as well as inverted arch of primary support reduces with the initial water content, and adds with burial depth of tunnel. The smaller the buried depth of tunnel, the larger the plastic zone area caused by the rock swelling. The expansion of the whole ring about rock has some inhibiting effect on the displacement about vault. After the rock swelling, the bending moments around the corner of primary support is the largest, which is the weakest position of the whole ring. After the installation of secondary support, the rock expands, then the safety factors of secondary support will be significantly reduced, and the weakest position is still at the corner of secondary support. The safety factors of secondary support decrease with the burial depth, but the decrease in amplitude is not large. The distribution rule about safety factors of secondary support structure under various buried depth conditions is basically the same, only the value difference, indicating that initial water contents show a great impact on safety factor. That is, the safety factors of secondary support structure are mainly affected by expansion force, not controlled by the ground pressure (burial depth).

CONCLUSION

Based on a tunnel project in expansive rock, using FLAC^{3D} software, adopting the principle

of temperature and humidity equivalence, and taking into account the impact of coupling efficiency of the buried depth of tunnel as well as the initial water contents of rock. The deformation law of rock and lining as well as the stability of secondary support are studied. The findings are listed below:

(1) Compared with burial depths of tunnel, the initial water contents about rock show an obvious impact on the development of plastic zone. For shallow tunnels with initial water contents of rock less than 10 %, the plastic zone of vault will penetrate to the surface after soaking expansion. The maximum development depth of plastic zone in vault is nearly three times of tunnel diameters, and the buried depth of tunnel inhibits the development of plastic zone to a certain extent.

(2) After rock swelling, the maximum bending moment of primary support occurs at the corner. The internal forces of tunnel support in expansive rock add with the buried depths, and when buried depths increase to 150 m, the buried depth has little effect on the internal forces increment of primary support. In the studied range of buried depth, the largest increment of bending moments is up to 456.4 kN·m.

(3) After the installation of secondary support, the rock swelling will lead to some significant reduction in the safety factor of secondary support, and the safety factor at the corner is the lowest. And safety factors of corner are not more than 2 after the buried depth of 150 m, which does not fulfill the need in the specification. The safety factors of secondary support structure are mainly influenced by the expansion force, not by the buried depth.

COMPETING INTERESTS

The authors have no relevant financial or non-financial interests to disclose.

DATA AVAILABILITY

All data, models, and code generated or used during the study appear in the submitted article.

REFERENCES

- [1] Wang, J.X., Liu, J.X., Liu, X.T., et al, 2017. In-site experiments on the swelling characteristics of a shield tunnel in expansive clay: A case study. *KSCE Journal of Civil Engineering*, Vol. 21, 976-986. <https://doi.org/10.1007/s12205-016-1333-4>
- [2] Zhang, H., Adoko, A.C., Meng, Z., et al, 2017. Mechanism of the mudstone tunnel failures induced by expansive clay minerals. *Geotechnical and Geological Engineering*, Vol. 35, 263-275. <https://doi.org/10.1007/s10706-016-0102-y>
- [3] Zhang, Y.T., Sun, X.L., Yang, B., et al, 2021. Influence of local expansion on safety of tunnel support. *Tunnel Construction*, Vol. 41, 306-312. <https://doi.org/10.3973/j.issn.2096-4498.2021.S2.039>
- [4] Xiang, Q.M., Gao, Y.Q., Su, J.X., et al, 2022. Strata subsidence characteristics of shield tunneling in coastal soft soil area. *Stavební obzor-Civil Engineering Journal*, Vol. 31, 444-455. <https://doi.org/10.14311/CEJ.2022.03.0033>
- [5] Zhao, J., Tan, Z.S., Wang, X., et al, 2022. Engineering characteristics of water-bearing weakly cemented sandstone and dewatering technology in tunnel excavation. *Tunnelling and Underground Space Technology*, Vol. 121, 104316. <https://doi.org/10.1016/j.tust.2021.104316>
- [6] Tang, Y.C., Huang, Z.H., Zhang, K., et al, 2014. Physical mechanical indexes and swelling property of weathered tertiary mudstone at shallow depth in Nanning. *Journal of Engineering Geology*, Vol. 22, 144-151. <https://doi.org/10.13544/j.cnki.jeg.2014.01.011>
- [7] Alonso, E.E., Berdugo, I.R., Ramon, A., 2013. Extreme expansive phenomena in anhydritic-gypsiferous claystone: the case of Lilla tunnel. *Géotechnique*, Vol. 63, 584-612. <https://doi.org/10.1680/geot.12.P.143>
- [8] Zhu, J.H., Zhang, H.Y., Ding, Z.N., et al, 2023. Stability analysis of tunnels in expansive soil using convergence-confinement and empirical methods. *Transportation Geotechnics*, Vol. 43, 101118.

<https://doi.org/10.1016/j.trgeo.2023.101118>

- [9] Ma, H., Chen, Y.L., Chang, L.X., et al, 2024. Assessing mechanical properties and response of expansive soft rock in tunnel excavation: a numerical simulation study. *Materials*, Vol. 17, 1747. <https://doi.org/10.3390/ma17081747>
- [10] Chen, Y.L., Liu, G.Y., Du, X., et al, 2020. Elastoplastic solution for a deep-buried tunnel considering swelling stress and dilatancy. *Rock and Soil Mechanics*, Vol. 41, 2525-2535. <https://doi.org/10.16285/j.rsm.2019.1799>
- [11] Chen, X., Wu, B.Y., Luo, W.J., et al, 2020. Stability of expansive soil tunnel surrounding rock under humidity condition. *Journal of Civil and Environmental Engineering*, Vol. 41, 2525-2535. <https://doi.org/10.11835/i.issn.2096-6717.2020.149>
- [12] Zhao, T., Liang, Q.G., Wu, F.Y., et al, 2022. Impact of base surrounding rock expansion on the mechanical characteristics of mudstone tunnel. *Journal of Southeast University*, Vol. 52, 538-546. <https://doi.org/10.3969/j.issn.1001-0505.2022.03.015>
- [13] Liao F.X., 2022. Instability Mechanism of Yuyuan tunnel based on expansion and strength deterioration effect. *Safety and Environmental Engineering*, Vol. 29, 33-45. <https://doi.org/10.13578/j.cnki.issn.1671-1556.20211374>
- [14] Zhang, C.B., Yu, Z.X., 2019. Study on impacts of softening and swelling of surrounding rocks on loosening pressure of rock mass. *Modern Tunnelling Technology*, Vol. 56, 50-56. <https://doi.org/10.13807/j.cnki.mtt.2019.02.008>
- [15] Fan, Q.Y., Liang, X., Han, J.S., 2020. Experimental study on saturation and swelling-shrinkage characteristics of unsaturated expansive rocks. *Chinese Journal of Rock Mechanics and Engineering*, Vol. 39, 45-56. <https://doi.org/10.13722/j.cnki.jrme.2019.0579>
- [16] Luo, Y., 2018. Elastoplastic analysis on strain softening and fracture expansion of roadway surrounding rock based on D - P criterion. *Journal of Safety Science and Technology*, Vol. 14, 108-113. <https://doi.org/10.11731/j.issn.1673-193x.2018.11.017>
- [17] Cao, P., 2023. Research on stability classification and support countermeasures of high-speed tunnel in expansive mudstone. Southwest Jiaotong University. (In Chinese)
- [18] Zhang, H.J., Liu, G.N., Chen, W., et al, 2024. Failure investigation of the tunnel lining in expansive mudstone-A case study. *Engineering Failure Analysis*, Vol. 158, 108003. <https://doi.org/10.1016/j.engfailanal.2024.108003>
- [19] National Railway Administration of the People's Republic of China. Code for rock and soil classification of railway engineering (TB 10077-2019). China Railway Publishing House, Beijing.
- [20] Liu, X.Z., Liu, F., Song, K.Z., 2022. Mechanism analysis of tunnel collapse in a soft-hard interbedded surrounding rock mass: A case study of the Yangshan Tunnel in China. *Engineering Failure Analysis*, Vol. 138, 106304. <https://doi.org/10.1016/j.engfailanal.2022.106304>
- [21] Zhao, J., Tan, Z., Zhang, B., et al, 2024. Stress-release technology and engineering application of advanced center drifts in a super-deep soft-rock tunnel: a case study of the Haba Snow Mountain Tunnel. *Rock Mechanics and Rock Engineering*, Vol. 57, 7103-7124. <https://doi.org/10.1007/s00603-024-03899-2>
- [22] Wu, B., Gao, B., Suo, X.M., et al, 2005. Mechanical simulation and analysis of construction behavior of urban metro tunnelling with small interval. *China Journal of Highway and Transport*, 84-89. <https://doi.org/10.19721/j.cnki.1001-7372.2005.03.019>
- [23] Zhang, S.K., Leng, X.L., Sheng, Q., 2020. Study of water swelling and softening characteristics of expansive rock. *Rock and Soil Mechanics*, Vol. 41, 561-570. <https://doi.org/10.16285/j.rsm.2019.0358>
- [24] Wang, L., Li, Z.Y., 2016. Triaxial compression test analysis of weakly cemented mudstone in west China. *Journal of Yangtze River Scientific Research Institute*, Vol. 33, 86-90. <https://doi.org/10.11988/ckyyb.20151116>
- [25] Yang, J.P., Fan, Y.H., 2016. The influence of temperature and humidity effect on water absorption softening of swelling rock. *Science Technology and Engineering*, Vol. 16, 259-263.
- [26] Zhang, K., Guo, J.T., Teng, T., 2022. Experimental study on water-softening and seepage characteristics of weakly cemented sandy mudstone: taking Shendong coal mining area as an example. *Coal Science and Technology*, Vol. 50, 195-201. <https://doi.org/10.13199/j.cnki.cst.2021-1216>
- [27] Fang, W., Zhang, H., Gao, S., et al, 2022. Mechanical characteristics and deformation law of tunnel in diatomite considering various softening conditions. *Stavební obzor-Civil Engineering Journal*, Vol. 31, 504-515.
- [28] Zeng, Z.Y., Xu, B.S., Hu, S.Q., et al., 2014. Numerical analysis of tunnel liner failure mechanism in expansive soil considering water-increased state. *Rock and Soil Mechanics*, Vol. 35, 871-880. <https://doi.org/10.16285/j.rsm.2014.03.045>
- [29] Xiong, J., 2021. Study on failure mechanism and support measures of high-speed rail tunnel in expansive rock. Southwest Jiaotong University. (In Chinese)
- [30] National Railway Administration of the People's Republic of China. Code for Design of Railway Tunnel (TB 10003-2016). China Railway Publishing House Co., Ltd, Beijing.